Conjugative Plasmid Transfer and Adhesion Dynamics in an *Escherichia coli* Biofilm[▽][†]

Cheryl-Lynn Y. Ong, Scott A. Beatson, Alastair G. McEwan, and Mark A. Schembri*

School of Chemistry and Molecular Biosciences, University of Queensland, Brisbane, Queensland 4072, Australia

A conjugative plasmid from the catheter-associated urinary tract infection strain *Escherichia coli* MS2027 was sequenced and annotated. This 42,644-bp plasmid, designated pMAS2027, contains 58 putative genes and is most closely related to plasmids belonging to incompatibility group X (IncX1). Plasmid pMAS2027 encodes two important virulence factors: type 3 fimbriae and a type IV secretion (T4S) system. Type 3 fimbriae, recently found to be functionally expressed in *E. coli*, played an important role in biofilm formation. Biofilm formation by *E. coli* MS2027 was specifically due to expression of type 3 fimbriae and not the T4S system. The T4S system, however, accounted for the conjugative ability of pMAS2027 and enabled a non-biofilm-forming strain to grow as part of a mixed biofilm following acquisition of this plasmid. Thus, the importance of conjugation as a mechanism to spread biofilm determinants was demonstrated. Conjugation may represent an important mechanism by which type 3 fimbria genes are transferred among the *Enterobacteriaceae* that cause device-related infections in nosocomial settings.

Bacterial biofilms are complex communities of bacterial cells living in close association with a surface (17). Bacterial cells in these protected environments are often resistant to multiple factors, including antimicrobials, changes in the pH, oxygen radicals, and host immune defenses (19, 38). Biofilm formation is a property of many bacterial species, and a range of molecular mechanisms that facilitate this process have been described (2, 3, 11, 14, 16, 29, 33, 34). Often, the ability to form a biofilm is dependent on the production of adhesins on the bacterial cell surface. In *Escherichia coli*, biofilm formation is enhanced by the production of certain types of fimbriae (e.g., type 1 fimbriae, type 3 fimbriae, F1C, F9, curli, and conjugative pili) (14, 23, 25, 29, 33, 39, 46), cell surface adhesins (e.g., autotransporter proteins such as antigen 43, AidA, TibA, EhaA, and UpaG) (21, 34, 35, 40, 43), and flagella (22, 45).

The close proximity of bacterial cells in biofilms creates an environment conducive for the exchange of genetic material. Indeed, plasmid-mediated conjugation in monospecific and mixed *E. coli* biofilms has been demonstrated (6, 18, 24, 31). The F plasmid represents the best-characterized conjugative system for biofilm formation by *E. coli*. The F pilus mediates adhesion to abiotic surfaces and stabilizes the biofilm structure through cell-cell interactions (16, 30). Many other conjugative plasmids also contribute directly to biofilm formation upon derepression of the conjugative function (16).

One example of a conjugative system employed by gram-negative *Enterobacteriaceae* is the type 4 secretion (T4S) system. The T4S system is a multisubunit structure that spans the cell envelope and contains a secretion channel often linked to a pilus or other surface filament or protein (8). The *Agrobacterium tumefaciens* VirB-VirD4 system is the archetypical T4S system and is encoded by 11 genes in the *virB* operon and one gene (*virD4*) in the *virD* operon (7, 8). Genes with strong homology to genes in the *virB* operon have also been identified on other conjugative plasmids. For example, the *pilX1* to *pilX11* genes on the *E. coli* R6K IncX plasmid and the *virB1* to *virB11* genes are highly conserved at the nucleotide level (28).

We recently described identification and characterization of the *mrk* genes encoding type 3 fimbriae in a uropathogenic strain of *E. coli* isolated from a patient with a nosocomial catheter-associated urinary tract infection (CAUTI) (29). The *mrk* genes were located on a conjugative plasmid (pMAS2027) and were strongly associated with biofilm formation. In this study we determined the entire sequence of plasmid pMAS2027 and revealed the presence of conjugative transfer genes homologous to the *pilX1* to *pilX11* genes of *E. coli* R6K (in addition to the *mrk* genes). We show here that biofilm formation is driven primarily by type 3 fimbriae and that the T4S apparatus is unable to mediate biofilm growth in the absence of the *mrk* genes. Finally, we demonstrate that conjugative transfer of pMAS2027 within a mixed biofilm confers biofilm formation properties on recipient cells due to acquisition of the type 3 fimbria-encoding *mrk* genes.

MATERIALS AND METHODS

Bacterial strains, plasmids, and growth conditions. The strains and plasmids used in this study are described in Table 1. Cells were routinely grown at 37°C using solid or liquid Luria-Bertani (LB) medium supplemented with appropriate antibiotics, unless otherwise stated. M9 minimal medium supplemented with 0.2% glucose and synthetic urine were prepared as previously described (26, 32).

DNA manipulations and genetic techniques. Plasmid DNA was isolated using QIAprep Spin Miniprep or Midiprep kits (Qiagen, Australia). Restriction endonucleases were used according to the manufacturer's specifications (New England Biolabs). PCR was performed using *Taq* polymerase according to the manufacturer's instructions (New England Biolabs). DNA sequencing was performed by the Australian Genome Research Facility. *E. coli* strain MS2027 was genetically marked by insertion of *gfp*mut3b* into the chromosomal attachment site of bacteriophage λ (*attB*) as previously described (34), which resulted in *E. coli* MS2091. Mutation of pMAS2027 was performed by performing λ-red-me-

TABLE 1. Bacterial strains and plasmids used in this study

Strain or plasmid	Description	Source or reference
E. coli strains		
DH5-α	Commercial laboratory *E. coli* cloning strain	Promega, United States
MS427	K-12 MG1655*flu*	21
MS661	MS427*recA*::*tet*	21
MS2027	*E. coli* CAUTI isolate	29
MS2091	MS2027 *attB*::*bla*-P$_{A1/04/03}$-*gfp*mut3b*-T$_0$;Gfp	This study
MS2103	MS2027(pMAS2027*pilX*::*kan*)	This study
MS2181	MS2027(pMAS2027*mrk*::*cam*)	This study
MS2183	MS2027(pMAS2027*mrk*::*cam pilX*::*kan*)	This study
MS2199	MS661 harboring pAR163	This study
MS2362	MS2027(pMAS2027*orf27*::*cam*)	This study
MS2517	MS2027(pMAS2027*mrk*::*gfp-kan*)	This study
MS2518	MS2027(pMAS2027*pilX*::*gfp-kan*)	This study
MS2519	MS2027(pMAS2027*orf27*::*gfp-kan*)	This study
Plasmids		
pAR163	dsRED2.T3-containing plasmid	34
pCO13	Kanamycin resistance gene inserted into HindIII-digested pKEN2	This study
pKD3	Deletion mutant template plasmid (*cam*)	12
pKD4	Deletion mutant template plasmid (*kan*)	12
pKEN2	*gfp*-containing plasmid	10
pMAS2027	*mrk*-containing conjugative plasmid isolated from MS2027	This study
pTW10	pGEM-T Easy with modified *kan* cassette without HindIII	43

diated homologous recombination as previously described (12), except that the *gfp-kan* mutants were constructed using pCO13 as the template DNA. Primers used in this study are described in Table 2. All deletion mutants were confirmed by PCR and subsequent DNA sequencing.

Sequencing and annotation of pMAS2027. Both strands of plasmid pMAS2027 were sequenced by employing a primer walking strategy. Primers were designed so that they read progressively outward from the *mrkA* and *mrkF* genes, until a complete, overlapping sequence was obtained. The DNA sequence was assembled using Contig Express (Invitrogen), and annotation was performed by using Vector NTi (Invitrogen) and Artemis (version 10) (5). BLASTn and BLASTp searches were performed using the National Center for Biotechnology Information website (1).

Plasmid mobilization study. Plasmid mobility was monitored by using filter paper bacterial conjugation as previously described (44). An overnight culture of the donor strain was concentrated 10-fold and left to stand at 37°C to allow growth of the sex pili. The donor and recipient (MS661) were then mixed at a ratio of 1:10 and then incubated on filter paper for 3 to 4 h. The filter paper mixture was then resuspended in LB medium, and dilutions were plated on LB agar containing tetracycline and kanamycin to select for transconjugants. Plates were incubated overnight at 37°C, and the plasmid conjugation efficiency was calculated by determining the ratio of transconjugant colonies to donor colonies.

Biofilm study. Biofilm formation on polyvinyl chloride (PVC) surfaces was monitored by using 96-well microtiter plates (Falcon) essentially as previously described (33). Briefly, cells were grown for 24 h in urine or M9 minimal medium (containing 0.2% glucose) at either 28°C or 37°C (statically or with shaking), washed to remove unbound cells, and stained with crystal violet. Quantification of bound cells was performed by addition of acetone-ethanol (20:80) and mea-

TABLE 2. Primers used in this study

| Primer	Description[a]	Sequence (5′–3′)
1293	50-bp overhang *mrk* knockout forward primer	TCTTCTCTCTGCAGCAATGGCAACCGCGTTTTTTGGCATGACTGCTGCCCGTGTAGGCTGGAGCTGCTTCG
1294	50-bp overhang *mrk* knockout reverse primer	GGTGTGAGCGGGATAGTTGTCTGAGTCACAGGCAGTTTCCTCTTCACCAGCATATGAATATCCTCCTTAG
1295	Screening forward primer (*mrk*)	GGCAGCATAACCGAACAAAT
1296	Screening reverse primer (*mrk*)	TAAATTTTCTGCGGCAAACC
1297	50-bp overhang *pilX* knockout forward primer	GTGGAATATTTATGTTATCTACTTCTACTTTTCTTGCGCTTGCCATGCAATGTGTAGGCTGGAGCTGCTTCG
1298	50-bp overhang *pilX* knockout reverse primer	TTTAATACTCATGATAATATCAATATTACTCAGTACACGTCTTAAAATGACATATGAATATCCTCCTTAG
1299	Screening forward primer (*pilX*)	CCGCAACGCAATGTACTCTA
1300	Screening reverse primer (*pilX*)	CGTTTTTCCGTTCAGGAAGT
1301	50-bp overhang Cm^r tag forward primer	AACGGGAAAACGAAAACAACAGATGAAAAGACACATACATTCAATACAGCGTGTAGGCTGGAGCTGCTTCG
1302	50-bp overhang Cm^r tag reverse primer	TTGCACTGGAGTTGATAATGGCCTCAATGCACAAATTGAGGTAAATTTATGTGTAGGCTGGAGCTGCTTCG
1303	Screening forward primer (tagging)	AGCAGTCCTGCAACCTAAGC
1304	Screening reverse primer (tagging)	TAATGGGCGTCCTAAACTGG
1305	GFP-*kan mrk* knockout forward primer	TCTTCTCTCTGCAGCAATGGCAACCGCGTTTTTTGGCATGACTGCTGCCCTAGGGCGAATTGACATTGTG
1306	GFP-*kan mrk* knockout reverse primer	GGTGTGAGCGGGATAGTTGTCTGAGTCACAGGCAGTTTCCTCTTCACCAGTGGACCAGTTGGTGATTTTG
1307	GFP-*kan pilX* knockout forward primer	GTGGAATATTTATGTTATCTACTTCTACTTTTCTTGCGCTTGCCATGCAATTAGGGCGAATTGACATTGTG
1308	GFP-*kan pilX* knockout reverse primer	TTTAATACTCATGATAATATCAATATTACTCAGTACACGTCTTAAAATGATGGACCAGTTGGTGATTTTG
1309	GFP-*kan* tagging forward primer	AACGGGAAAACGAAAACAACAGATGAAAAGACACATACATTCAATACAGCTAGGGCGAATTGACATTGTG
1310	GFP-*kan* tagging reverse primer	TTGCACTGGAGTTGATAATGGCCTCAATGCACAAATTGAGGTAAATTTATTGGACCAGTTGGTGATTTTG
pCO_F	pCO13 internal screening forward primer (*kan* region)	CGAAAGATCCCAACGAAAAG
pCO13-R2	pCO13 internal screening reverse primer (GFP region)	TCGATAGATTGTCGCACCTG
pCO13-F3	pCO13 external screening forward primer (GFP region)	CAGCAACACCTTCTTCACGA
pCO13-R3	pCO13 external screening reverse primer (*kan* region)	TCACCTTCACCCTCTCCACT

[a] GFP, green fluorescent protein.
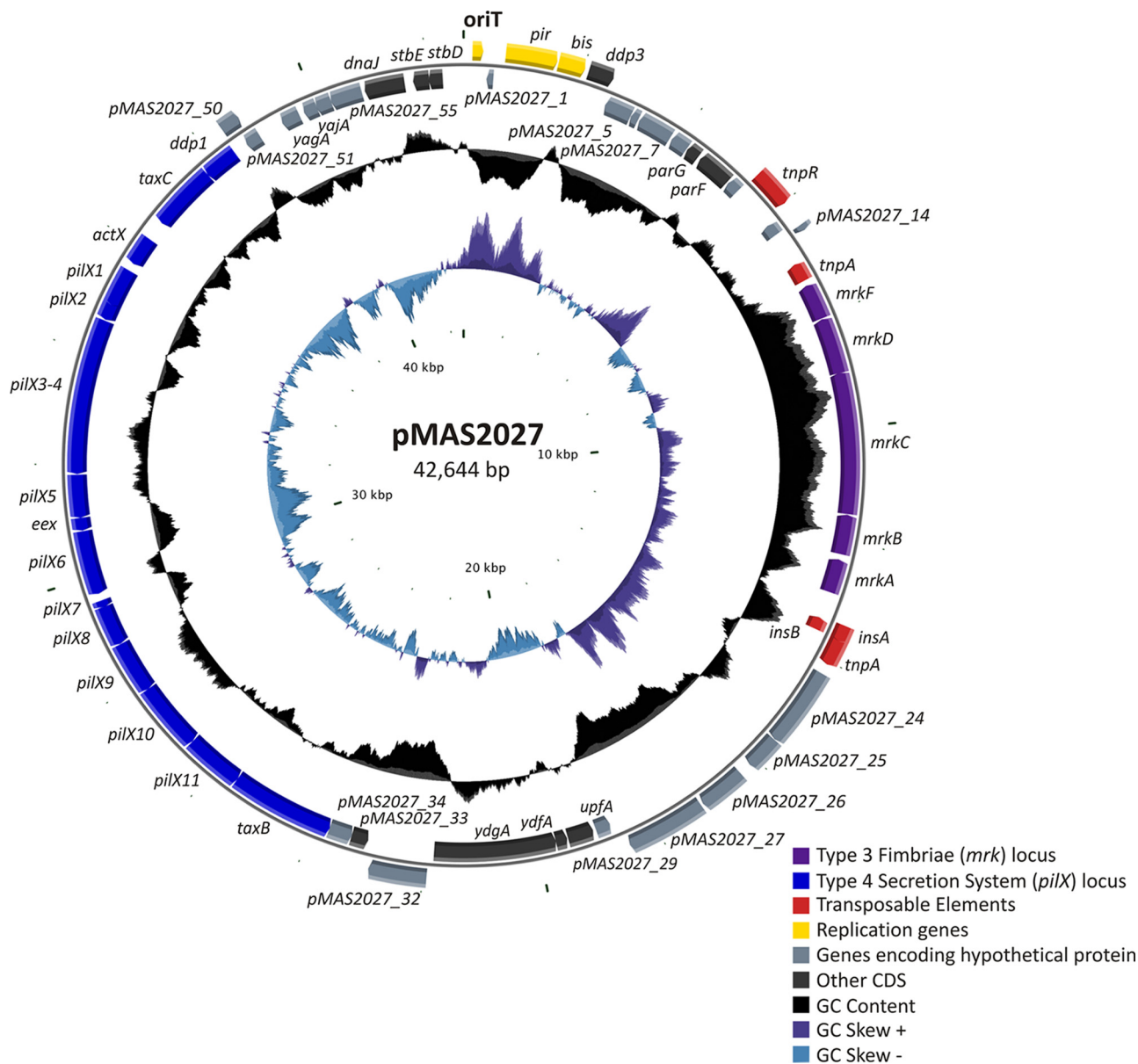
FIG. 1. Circular diagram of plasmid pMAS2027. The outer circle indicates (to scale) the genetic organization of ORFs within the plasmid. The direction of transcription of each ORF is indicated. The middle circle indicates the G+C content, and the inner circle indicates the GC skew. Genes are color coded as indicated. The image was constructed using cgview (37). CDS, coding sequences.

surement of the dissolved crystal violet using the optical density at 595 nm. Flow chamber biofilm experiments were performed as previously described (21). Briefly, biofilms were allowed to form on glass surfaces in a multichannel flow system that permitted online monitoring of community structures. Flow cells were inoculated with overnight cultures that were standardized using the optical density at 600 nm and were prepared in M9 medium. Biofilm development was monitored by confocal scanning laser microscopy at 16 to 24 h after inoculation. All experiments were performed in triplicate. In the flow chamber experiments with mixed biofilms, the donor and recipient strains were incubated for 6 h before they were subjected to the medium flow. Biofilm development was monitored by confocal scanning laser microscopy at 16 and 40 h after inoculation. All experiments were performed in triplicate. Both single-strain biofilm and mixed-biofilm flow chamber experiments were done using M9 minimal medium supplemented with 100 µg/µl ampicillin.

SEM. Scanning electron microscopy (SEM) was performed essentially as previously described (29). Cells were grown as described above for the biofilm study on PVC surfaces, except that the experiment was performed using a 12-well

microtiter plate (Griener bio-one) with a polystyrene disk placed at the bottom. The disk was fixed with 3% glutaraldehyde in 0.1 M cacodylate buffer and postfixed with 1% osmium tetroxide in 0.1 M cacodylate buffer. The sample was then infiltrated with glycerol and frozen in liquid nitrogen. The sample was freeze substituted in 100% ethanol containing a molecular sieve and incubated at −80°C for 10 h; then the temperature was increased from −80°C to −20°C over a 10-h period, and the sample was critical point dried. The sample was then mounted on carbon tabs and sputter coated with platinum at 15 mA for 120 s.

Statistical analysis. Differences in plasmid conjugation efficiency between pMAS2027mrk::kan and pMAS2027orf24::cam were determined by using a t test (with two samples assuming unequal variances). Differences in biofilm formation were analyzed using the analysis of variance single-factor test, and values were compared with values obtained for *E. coli* MS2027 (wild type) or *E. coli* MS2362 (MS2027::cam) (Minitab 15 statistical software).

Nucleotide sequence accession number. The pMAS2027 plasmid sequence has been deposited in the GenBank database under accession number FJ666132.
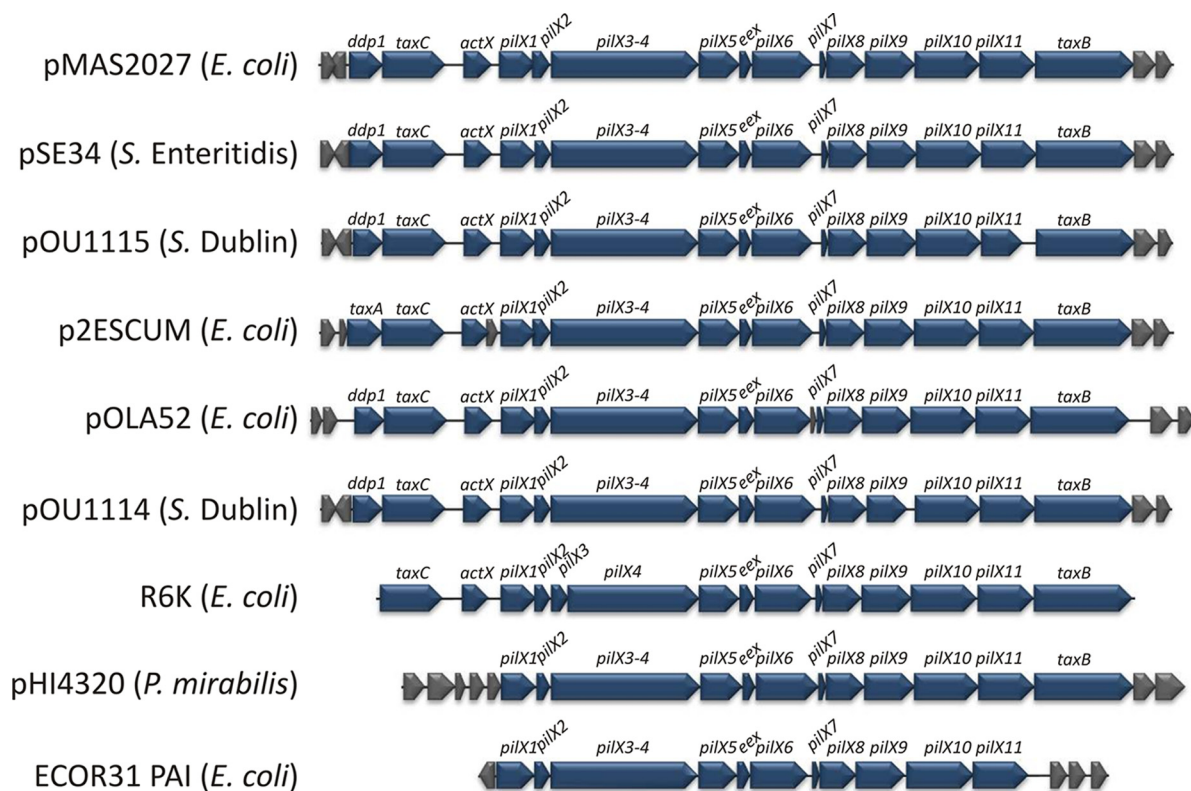
FIG. 2. Physical map comparing the genes encoding the T4S system (and adjacent genes) in plasmid pMAS2027 to the corresponding regions in plasmids pSE34 (*Salmonella* serovar Enteritidis; EU219533), pOU1115 (*Salmonella* serovar Dublin; DQ115388), p2ESCUM (*E. coli*; CU928149), pOLA52 (*E. coli*; EU370913), pOU1114 (*Salmonella* serovar Dublin; DQ115387), R6K (*E. coli*; AJ006342), and pHI4320 (*P. mirabilis*; AM942760) and the pathogenicity island (PAI) in *E. coli* ECOR31 (AY233333). The genes encoding the T4S system are blue and include *ddp1* (*taxA*), *taxC*, *actX*, *pilX1* to *pilX11*, and *taxB*. Adjacent genes (gray) encode hypothetical proteins with unknown functions. No sequence information is available for genes outside the T4S system gene cluster in *E. coli* R6K. The direction of transcription of each gene is indicated.

RESULTS

Complete nucleotide sequence of pMAS2027. Plasmid pMAS2027 was determined to be a 42,644-bp circular plasmid with a G+C content of 43.43% (Fig. 1). Bioinformatic analysis predicted the presence of 58 open reading frames (ORFs), which represent 88.83% of the total plasmid DNA. Plasmid pMAS2027 is most closely related to the IncX group of plasmids, a narrow-host-range family of conjugative plasmids commonly found in the family *Enterobacteriaceae* (13). The backbone structure of pMAS2027 contains genes associated with plasmid stability and partitioning, as well as a 14,628-kb region comprising genes predicted to encode a T4S system (Fig. 1). This region includes the *pilX1* to *pilX11* genes analogous to the genes described for R6K (28) and most likely involved in conjugative DNA transfer. pMAS2027 also contains the *mrkABCDF* genes (encoding type 3 fimbriae). The *mrk* genes are located on a 5,536-bp segment and have an overall G+C content of 56.6%. Genes predicted to encode proteins associated with transposition are located both upstream (*tnpR* and *tnpA*) and downstream (*insA*, *insB*, and *tnpA*) of the *mrk* cluster, suggesting that the *mrk* genes are located on a mobile genetic element. A summary of each ORF of pMAS2027, including the predicted function of each encoded protein, is shown in Table 1S in the supplemental material. No genes were predicted to encode proteins associated with antibiotic resistance. The remainder of our study focused on the relative contributions of the *mrk* and *pilX1* to *pilX11* genes to biofilm formation and conjugative transfer.

Bioinformatic analysis of the conjugative transfer locus of plasmid pMAS2027. The *pilX1* to *pilX11* genes of pMAS2027 are 43% identical at the nucleotide sequence level to the *virB1* to *virB11* genes of the archetypical transferred DNA transfer system of the plant pathogen *A. tumefaciens* (42). These genes have also been identified on conjugative plasmids isolated from other *Enterobacteriaceae*, including *Salmonella enterica* serovar Enteritidis, *S. enterica* serovar Dublin, *Proteus mirabilis*, and other *E. coli* strains (Fig. 2). The *pilX1* to *pilX11* regions of three plasmids (pSE34 from *Salmonella* serovar Enteritidis, pOU1115 from *Salmonella* serovar Dublin, and p2ESCUM from *E. coli*) share the strongest overall sequence identity with the *pilX1* to *pilX11* genes of pMAS2027 (Table 3). The sequences of two other plasmids (pOLA52 from *E. coli* and pOU1114 from *Salmonella* serovar Dublin) were also highly conserved in this region, except for the *eex* and *pilX6* genes. The nucleotide sequences of the *pilX1* to *pilX11* genes of pMAS2027, R6K (an archetypical *E. coli* IncX plasmid), and pHI4320 (*P. mirabilis*) were more divergent (Table 3). Despite this, the genetic organization of the *pilX1* to *pilX11* (and adjacent) genes on pMAS2027 and a number of other conjugative plasmids is highly conserved (Fig. 2).

TABLE 3. Comparison of the *E. coli* plasmid pMAS2027 T4S system protein and nucleotide sequences with the corresponding sequences from other T4S system conjugative plasmids

T4S system protein	% Amino acid identity (% nucleotide sequence conservation)								
	pSE34	pOU1115	p2ESCUM	pOLA52	pOU1114	R6K	pHI4320	ECOR31 pathogenicity island	pTi[b]
Ddp1	97 (98)	87 (88)	85 (89)	88 (88)	88 (88)	NA[c]	NA	NA	NA
TaxC	97 (98)	97 (97)	97 (97)	98 (98)	97 (98)	77 (71)	NA	NA	NA
ActX	99 (100)	99 (100)	29 (48)	99 (100)	99 (100)	25 (47)	NA	NA	NA
PilX1/VirB1	93 (93)	94 (94)	93 (93)	94 (94)	93 (93)	62 (64)	44 (53)	41 (47)	22 (42)
PilX2/VirB2	89 (90)	89 (89)	91 (93)	89 (89)	89 (90)	76 (68)	29 (42)	20 (42)	13 (45)
PilX3- PilX4/VirB3-VirB4[a]	99 (99)	100 (99)	99 (99)	100 (99)	99 (99)	80 (74)	63 (63)	42 (53)	24 (47)
PilX5/VirB5	100 (100)	98 (98)	98 (98)	93 (95)	100 (100)	63 (67)	48 (60)	27 (49)	11 (46)
Eex	97 (100)	97 (100)	97 (100)	35 (45)	49 (56)	28 (46)	43 (57)	33 (48)	NA
PilX6/VirB6	99 (100)	99 (99)	98 (99)	68 (69)	81 (79)	58 (61)	54 (58)	30 (46)	13 (39)
PilX7/VirB7	100 (100)	100 (100)	100 (100)	100 (100)	100 (100)	72 (77)	40 (61)	33 (51)	18 (36)
PilX8/VirB8	99 (99)	99 (100)	99 (100)	99 (100)	99 (99)	75 (72)	45 (54)	33 (46)	17 (43)
PilX9/VirB9	98 (98)	99 (100)	98 (99)	100 (100)	77 (79)	80 (74)	54 (60)	39 (54)	23 (48)
PilX10/VirB10	99 (99)	100 (100)	100 (98)	100 (100)	100 (100)	63 (65)	50 (59)	42 (55)	23 (44)
PilX11/VirB11	98 (98)	72 (74)	98 (97)	99 (100)	100 (100)	73 (71)	59 (65)	43 (53)	26 (47)
TaxB	99 (99)	99 (99)	98 (96)	99 (100)	99 (99)	78 (70)	72 (67)	NA	NA
Hyp	93 (95)	96 (98)	96 (98)	100 (100)	96 (98)	NA	44 (57)	NA	NA
Hyp	77 (79)	85 (86)	92 (90)	100 (100)	85 (86)	NA	NA	NA	NA

[a] *pilX3* and *pilX4* and *virB3* and *virB4* in R5K and pTi are separate genes, but in all other plasmids they are fused in one ORF.
[b] pTi contains the *virB* operon, which was compared to the *pilX* operon of pMAS2027.
[c] NA, not applicable.

The *pilX* locus promotes conjugative transfer of plasmid pMAS2027. To demonstrate the function of the *pilX1* to *pilX11* genes, the entire segment was deleted by λ-red-mediated homologous recombination and replaced by insertion of a kanamycin resistance gene (to generate plasmid pMAS2027*pilX*::*kan*). Plasmid pMAS2027*pilX*::*kan* could not be mobilized into a recipient *E. coli* strain, confirming the function of the *pilX1* to *pilX11* genes in conjugative transfer. To examine whether type 3 fimbriae (encoded by the *mrkABCDF* genes on pMAS2027) also contribute to the efficiency of conjugative transfer, we constructed two additional plasmids: pMAS2027*mrk*::*kan* and pMAS2027*orf27*::*cam*. Plasmid pMAS2027*orf27*::*cam* contained a gene encoding resistance to chloramphenicol inserted into *orf27* (which encodes a hypothetical protein of unknown function) and thus served as a control. The frequency of conjugative transfer, calculated by determining the number of transconjugants per donor, was 0.0064 for pMAS2027*orf27*::*cam*, compared to 0.032 for pMAS2027*mrk*::*kan* ($P < 0.05$). Thus, the lack of type 3 fimbriae resulted in a fivefold increase in conjugative plasmid transfer.

Type 3 fimbriae, but not T4S pili, contribute to biofilm formation. The contributions of type 3 fimbriae and T4S pili to biofilm growth were examined by using MS2027 harboring either pMAS2027*mrk*::*kan*, pMAS2027*pilX*::*kan*, or pMAS2027*orf27*::*cam* and performing two dynamic biofilm assays. First, we used a PVC microtiter plate assay and showed that type 3 fimbriae, but not T4S pili, promote biofilm formation after growth in M9 minimal medium and in urine (Fig. 3). Next, we tested the ability of the same strains to promote biofilm formation in a continuous-flow chamber. Consistent with the results of our microtiter plate assay, MS2072 harboring pMAS2027*orf27*::*cam* and MS2072 harboring pMAS2027*pilX*::*kan* produced equivalent, strong biofilms that were approximately 20 μm deep, while MS2072 harboring pMAS2027*mrk*::*kan* was unable to form a

biofilm (Fig. 4). An additional plasmid construct with both the *mrk* and *pilX* genes deleted (pMAS2027*mrk*::*kan pilX*::*cam*) was also examined and did not mediate biofilm growth. Thus, although plasmid pMAS2027 encodes the capacity to produce conjugative T4S pili, these pili did not contribute to biofilm formation in these experiments.

Transfer of the *mrk* genes via conjugation in an evolving mixed biofilm. A further three deletion mutants were constructed by replacing the *mrk*, *pilX*, and *orf27* genes on pMAS2027 with *gfp* and a kanamycin resistance gene, tagging pMAS2027 with *gfp* in the process. MS2027 cells harboring plasmid pMAS2027*mrk*::*gfp-kan*, pMAS2027*pilX*::*gfp-kan*, or pMAS2027*orf27*::*gfp-kan* were examined for the ability to form a mixed biofilm in the continuous-flow chamber system with *E. coli* K-12 strain MS2199, a non-biofilm-forming strain tagged with the *rfp* gene. Biofilm formation was assessed by performing scanning laser confocal microscopy at 16 h, 30 h, and 40 h after inoculation. *E. coli* MS2199 was unable to form a biofilm at all three time points when it was alone and when it was grown in a coculture with MS2027(pMAS2027*mrk*::*gfp-kan*) or MS2027(pMAS2027*pilX*::*gfp-kan*) (Fig. 5A). However, when *E. coli* MS2199 was grown in a coculture with MS2027 (pMAS2027*orf27*::*gfp-kan*), a mixed biofilm consisting of MS2027(pMAS2027*orf27*::*gfp-kan*) cells (green) and transconjugant MS2199 cells (yellow) formed (Fig. 5A). Close examination of the mixed biofilm (magnification, ×100) revealed regions with a mixture of green and yellow cells, suggesting that there was conjugative transfer within the evolving biofilm. Taken together, the data demonstrate that conjugative transfer of pMAS2027*orf27*::*gfp-kan* from MS2027 to MS2199 enabled MS2199 transconjugant cells to form a strong biofilm due to production of type 3 fimbriae. No red-tagged MS2199 cells were observed in the mixed biofilm. When the mixed biofilm containing MS2199 and MS2027(pMAS2027*orf27*::*gfp-kan*)
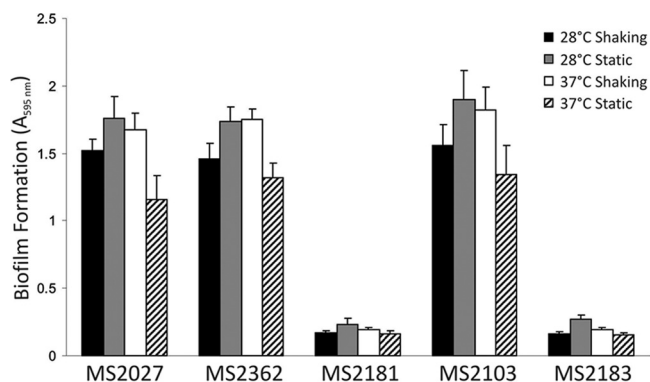
FIG. 3. Biofilm formation by *E. coli* MS2027 and derivatives. Strains were grown in urine for 16 h in PVC microtiter plates under various conditions, as indicated. Biofilm formation was quantified by staining adhered cells with 0.1% crystal violet, resuspending them in ethanol-acetate (80:20), and measuring the absorbance at 595 nm. The results are the averages and standard deviations of three independent experiments. The data are the results for MS2027, MS2362 [MS2027(pMAS2027*orf27*::*cam*)], MS2181 [MS2027(pMAS2027*mrk*::*cam*)], MS2103 [MS2027(pMAS2027*pilX*::*kan*)], and MS2183 [MS2027(pMAS2027*mrk*::*cam*, *pilX*::*kan*)].

was viewed with an SEM, T4S pilus-like structures linking cells within the biofilm were observed (Fig. 5B). Thus, it is possible that the T4S pili encoded on pMAS2027 contribute to the structural composition of a mixed biofilm both directly and through their ability to transfer the type 3 fimbria-encoding *mrk* genes to recipient cells.

DISCUSSION

Biofilm formation by uropathogenic *E. coli* is mediated by a range of cell surface factors, including fimbriae, flagella, and adhesins. Often, the genes encoding these factors are located on mobile genetic elements, such as plasmids, transposons, and pathogenicity islands. Here we determined the complete nucleotide sequence of a conjugative plasmid isolated from a strain of uropathogenic *E. coli* that caused CAUTI and defined the properties of this plasmid that are associated with biofilm growth.

Plasmid pMAS2027 is most closely related to conjugative plasmids belonging to the IncX group (36), and its nucleotide sequence strongly suggested that it belonged to IncX1, a subset of this group (20). The genetic organization of pMAS2027 is similar to that previously described for several characterized virulence plasmids from *S. enterica* (9, 15, 41). Indeed, of the 58 ORFs identified on pMAS2027, 40 (69%) exhibit the strongest nucleotide sequence similarity to *S. enterica* genes. The major genetic load region of pMAS2027 comprised the *mrk* genes (encoding type 3 fimbriae), which appear to be located on a mobile genetic element. Recently, a large conjugative plasmid (pOLA52) isolated from swine manure that also contains both the *mrkABCDF* and *pilX1* to *pilX11* genes was described (27).
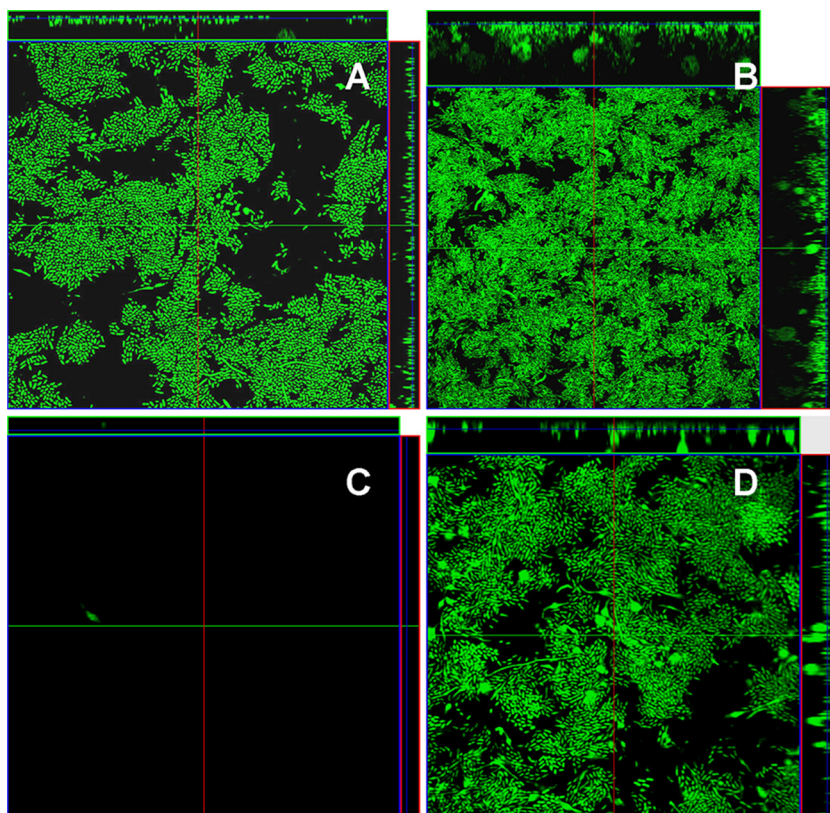

FIG. 4. Flow chamber biofilm formation for (A) *E. coli* MS2091 (MS2027 *attB*::*bla*-P$_{A1/04/03}$-*gfp*mut3b*-T$_0$;Gfp), (B) MS2519 [MS2027 (pMAS2027*orf27*::*gfp-kan*)], (C) MS2517 [MS2027(pMAS2027*mrk*::*gfp-kan*)], and (D) MS2518 [MS2027(pMAS2027*pilX*::*gfp-kan*)]. Biofilm development was monitored by confocal scanning laser microscopy 24 h after inoculation. The large micrographs show horizontal sections. To the right of and above each large image are images of the *yz* plane and the *xz* plane, respectively, obtained at the positions indicated by the lines.
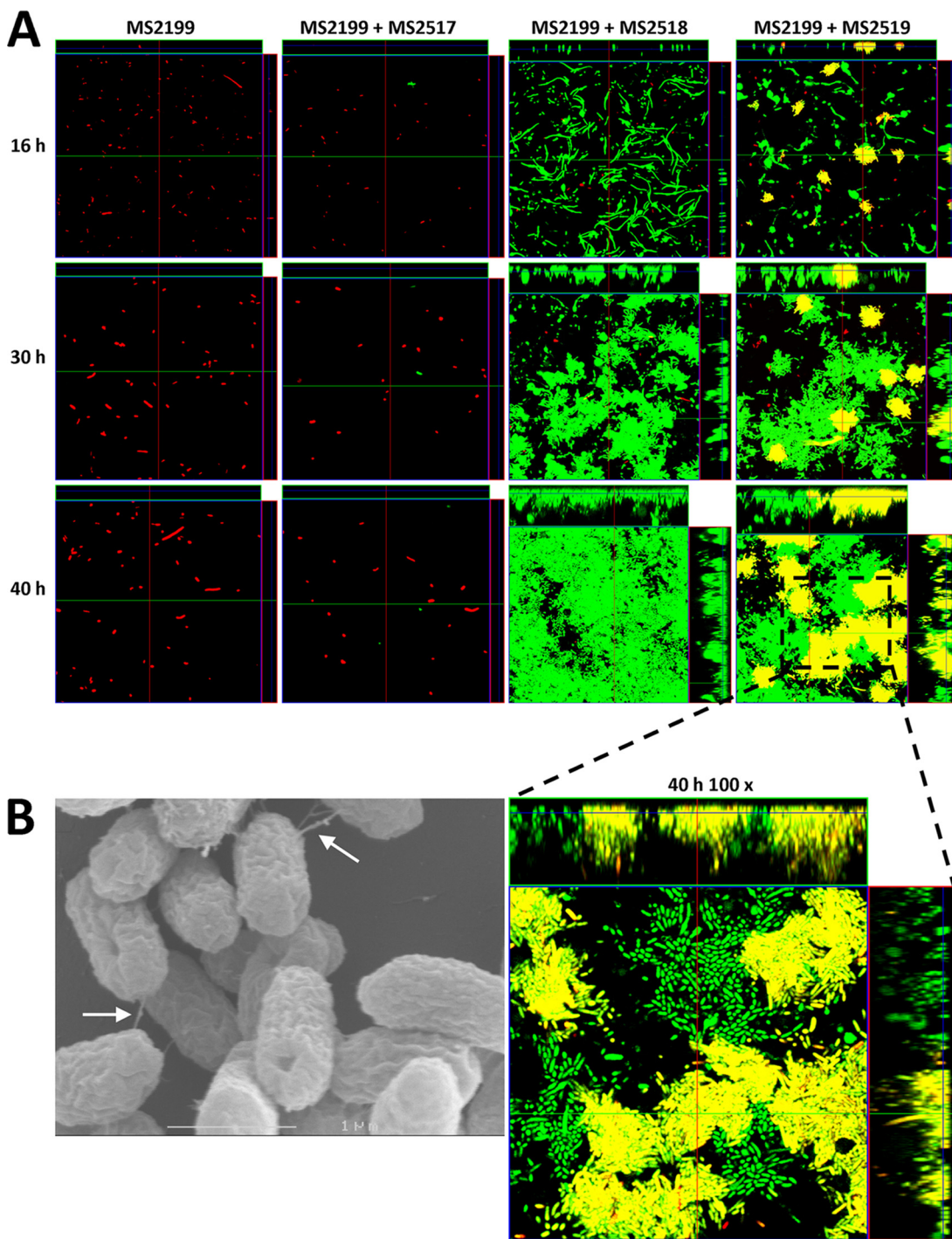
FIG. 5. (A) Flow chamber biofilm formation for *E. coli* MS2199 (Rfp⁺) and mixed cultures of *E. coli* MS2199 (Rfp⁺) and MS2517 [MS2027(pMAS2027*mrk*::*gfp-kan*)] (Gfp⁺), MS2199 (Rfp⁺) and MS2518 [MS2027(pMAS2027*pilX*::*gfp-kan*)] (Gfp⁺), and MS2199 (Rfp⁺) and MS2519 [MS2027(pMAS2027*orf27*::*gfp-kan*)] (Gfp⁺). Magnification, ×40. Biofilm development was monitored by confocal scanning laser microscopy at 16 h, 30 h, and 40 h after inoculation. The micrographs show horizontal sections. To the right of and above each large panel are images of the *yz* plane and the *xz* plane, respectively, obtained at the positions indicated by the lines. The largest micrograph shows a higher magnification (×100) of a defined region of the MS2199-MS2519 mixed biofilm. (B) SEM micrograph of a mixed MS2199-MS2519 microtiter plate biofilm. Putative T4S pilus structures are indicated by arrows.

The *mrkABCDF* genes of pOLA52 are flanked by transposon-like sequences, and the nucleotide sequences of these genes are >94% identical to the nucleotide sequences of the *mrkABCDF* genes of pMAS2027. A comparison of the *pilX1* to *pilX11* genes of the two plasmids also revealed a high degree of nucleotide sequence conservation, except for the *eex* and *pilX6* genes. Although pOLA52 is approximately 10 kb larger than pMAS2027 and contains genes that impart multidrug resis-

tance, the similarity between the backbone sequences of the two plasmids is striking considering that the plasmids were identified in strains isolated from two very different environments (i.e., swine manure and the urine of a patient with CAUTI).

The ability to produce type 3 fimbriae was an absolute requirement for biofilm growth of *E. coli* MS2027. No biofilm formation was observed with mutants that lacked the *mrkABCDF* genes but retained the ability to produce conjugative T4S pili. Thus, unlike the F pilus (16, 30), T4S pili do not mediate binding to abiotic surfaces and do not promote biofilm formation. Although the role of type 3 fimbriae in biofilm formation was consistent in previous studies performed with plasmid pOLA52 (4), we found that deletion of *mrkABCDF* resulted in a fivefold increase in the conjugation efficiency of pMAS2027. This finding is in contrast to the results of studies performed with pOLA52, where mutation of the *mrkC* gene (which abrogates production of type 3 fimbriae) caused a dramatic reduction in conjugation efficiency (4). It is possible that this discrepancy is due to differences in the makeup of other cell surface components that might interfere with this process between the *E. coli* strains harboring pMAS2027 and pOLA52.

Mixed-culture flow chamber assays were employed to examine the contribution of conjugative plasmid transfer to biofilm development. Maintenance of transconjugant MS2199(pMAS2027*orf27::cam*) cells within a biofilm was dependent on the production of type 3 fimbriae. Thus, the genetic load of pMAS2027 (*mrkABCDF*) defined its ability to spread laterally within the biofilm. Genes encoding type 3 fimbriae have been identified in many gram-negative uropathogens, including *Klebsiella* spp., *E. coli*, *Enterobacter* spp., *P. mirabilis*, *Serratia* spp., *Yersinia* spp., and *Providentia* spp. It is likely that the widespread occurrence of type 3 fimbria-encoding genes in these pathogens is associated with plasmid transfer within biofilms in the hospital setting.

ACKNOWLEDGMENTS

REFERENCES

1. **Altschul, S. F., W. Gish, W. Miller, E. W. Myers, and D. J. Lipman.** 1990. Basic local alignment search tool. J. Mol. Biol. **215:**403–410.
2. **Balestrino, D., J. A. J. Haagensen, C. Rich, and C. Forestier.** 2005. Characterization of type 2 quorum sensing in *Klebsiella pneumoniae* and relationship with biofilm formation. J. Bacteriol. **187:**2870–2880.
3. **Barnhart, M. M., and M. R. Chapman.** 2006. Curli biogenesis and function. Annu. Rev. Microbiol. **60:**131–147.
4. **Burmolle, M., M. L. Bahl, L. B. Jensen, S. J. Sorensen, and L. H. Hansen.** 2008. Type 3 fimbriae, encoded by the conjugative plasmid pOLA52, enhance biofilm formation and transfer frequencies in Enterobacteriaceae strains. Microbiology **154:**187–195.
5. **Carver, T., M. Berriman, A. Tivey, C. Patel, U. Bohme, B. G. Barrell, J. Parkhill, and M. A. Rajandream.** 2008. Artemis and ACT: viewing, annotating and comparing sequences stored in a relational database. Bioinformatics **24:**2672–2676.
6. **Christensen, B. B., C. Sternberg, J. B. Andersen, L. Eberl, S. Moller, M. Givskov, and S. Molin.** 1998. Establishment of new genetic traits in a microbial biofilm community. Appl. Environ. Microbiol. **64:**2247–2255.
7. **Christie, P. J.** 1997. *Agrobacterium tumefaciens* T-complex transport apparatus: a paradigm for a new family of multifunctional transporters in eubacteria. J. Bacteriol. **179:**3085–3094.
8. **Christie, P. J., K. Atmakuri, V. Krishnamoorthy, S. Jakubowski, and E. Cascales.** 2005. Biogenesis, architecture, and function of bacterial type IV secretion systems. Annu. Rev. Microbiol. **59:**451–485.
9. **Chu, C. S., Y. Feng, A. C. Chien, S. N. Hu, C. H. Chu, and C. H. Chiu.** 2008. Evolution of genes on the Salmonella virulence plasmid phylogeny revealed from sequencing of the virulence plasmids of S. enterica serotype Dublin and comparative analysis. Genomics **92:**339–343.
10. **Cormack, B. P., R. H. Valdivia, and S. Falkow.** 1996. FACS-optimized mutants of the green fluorescent protein (GFP). Gene **173:**33–38.
11. **Cucarella, C., C. Solano, J. Valle, B. Amorena, I. Lasa, and J. R. Penades.** 2001. Bap, a *Staphylococcus aureus* surface protein involved in biofilm formation. J. Bacteriol. **183:**2888–2896.
12. **Datsenko, K. A., and B. L. Wanner.** 2000. One-step inactivation of chromosomal genes in Escherichia coli K-12 using PCR products. Proc. Natl. Acad. Sci. USA **97:**6640–6645.
13. **Datta, N., and V. M. Hughes.** 1983. Plasmids of the same Inc groups in enterobacteria before and after the medical use of antibiotics. Nature **306:**616–617.
14. **Di Martino, P., N. Cafferini, B. Joly, and A. Darfeuille-Michaud.** 2003. Klebsiella pneumoniae type 3 pili facilitate adherence and biofilm formation on abiotic surfaces. Res. Microbiol. **154:**9–16.
15. **Fierer, J., L. Eckmann, F. Fang, C. Pfeifer, B. B. Finlay, and D. Guiney.** 1993. Expression of the *Salmonella* virulence plasmid gene *spvB* in cultured macrophages and nonphagocytic cells. Infect. Immun. **61:**5231–5236.
16. **Ghigo, J. M.** 2001. Natural conjugative plasmids induce bacterial biofilm development. Nature **412:**442–445.
17. **Hall-Stoodley, L., J. W. Costerton, and P. Stoodley.** 2004. Bacterial biofilms: from the natural environment to infectious diseases. Nat. Rev. Microbiol. **2:**95–108.
18. **Hausner, M., and S. Wuertz.** 1999. High rates of conjugation in bacterial biofilms as determined by quantitative in situ analysis. Appl. Environ. Microbiol. **65:**3710–3713.
19. **Jefferson, K. K.** 2004. What drives bacteria to produce a biofilm? FEMS Microbiol. Lett. **236:**163–173.
20. **Jones, C. S., D. J. Osborne, and J. Stanley.** 1993. Molecular comparison of the IncX plasmids allows division into IncX1 and IncX2 subgroups. J. Gen. Microbiol. **139:**735–741.
21. **Kjaergaard, K., M. A. Schembri, C. Ramos, S. Molin, and P. Klemm.** 2000. Antigen 43 facilitates formation of multispecies biofilms. Environ. Microbiol. **2:**695–702.
22. **Lane, M. C., V. Lockatell, G. Monterosso, D. Lamphier, J. Weinert, J. R. Hebel, D. E. Johnson, and H. L. T. Mobley.** 2005. Role of motility in the colonization of uropathogenic *Escherichia coli* in the urinary tract. Infect. Immun. **73:**7644–7656.
23. **Lasaro, M. A., N. Salinger, J. Zhang, Y. T. Wang, Z. T. Zhong, M. Goulian, and J. Zhu.** 2009. F1C fimbriae play an important role in biofilm formation and intestinal colonization by the *Escherichia coli* commensal strain Nissle 1917. Appl. Environ. Microbiol. **75:**246–251.
24. **Lebaron, P., P. Bauda, M. C. Lett, Y. Duval-Iflah, P. Simonet, E. Jacq, N. Frank, B. Roux, B. Baleux, G. Faurie, J. C. Hubert, P. Normand, D. Prieur, S. Schmitt, and J. C. Block.** 1997. Recombinant plasmid mobilization between E. coli strains in seven sterile microcosms. Can. J. Microbiol. **43:**534–540.
25. **Luo, H. L., K. Wan, and H. H. Wang.** 2005. High-frequency conjugation system facilitates biofilm formation and pAMβ1 transmission by *Lactococcus lactis*. Appl. Environ. Microbiol. **71:**2970–2978.
26. **Martino, P. D., R. Fursy, L. Bret, B. Sundararaju, and R. S. Phillips.** 2003. Indole can act as an extracellular signal to regulate biofilm formation of Escherichia coli and other indole-producing bacteria. Can. J. Microbiol. **49:**443–449.
27. **Norman, A., L. H. Hansen, Q. X. She, and S. J. Sorensen.** 2008. Nucleotide sequence of pOLA52: a conjugative IncX1 plasmid from Escherichia coli which enables biofilm formation and multidrug efflux. Plasmid **60:**59–74.
28. **Nunez, B., P. Avila, and F. de la Cruz.** 1997. Genes involved in conjugative DNA processing of plasmid R6K. Mol. Microbiol. **24:**1157–1168.
29. **Ong, C. L. Y., G. C. Ulett, A. N. Mabbett, S. A. Beatson, R. I. Webb, W. Monaghan, G. R. Nimmo, D. F. Looke, A. G. McEwan, and M. A. Schembri.** 2008. Identification of type 3 fimbriae in uropathogenic *Escherichia coli* reveals a role in biofilm formation. J. Bacteriol. **190:**1054–1063.
30. **Reisner, A., J. A. Haagensen, M. A. Schembri, E. L. Zechner, and S. Molin.** 2003. Development and maturation of Escherichia coli K-12 biofilms. Mol. Microbiol. **48:**933–946.
31. **Reisner, A., B. M. Holler, S. Molin, and E. L. Zechner.** 2006. Synergistic effects in mixed *Escherichia coli* biofilms: conjugative plasmid transfer drives biofilm expansion. J. Bacteriol. **188:**3582–3588.
32. **Sambrook, J., and D. W. Russell.** 2001. Molecular cloning: a laboratory manual, 3rd ed., vol. 1. Cold Spring Harbor Laboratory Press, Cold Spring Harbor, NY.
33. **Schembri, M. A., and P. Klemm.** 2001. Biofilm formation in a hydrodynamic environment by novel FimH variants and ramifications for virulence. Infect. Immun. **69:**1322–1328.
34. **Sherlock, O., M. A. Schembri, A. Reisner, and P. Klemm.** 2004. Novel roles for the AIDA adhesin from diarrheagenic *Escherichia coli*: cell aggregation and biofilm formation. J. Bacteriol. **186:**8058–8065.
35. **Sherlock, O., R. M. Vejborg, and P. Klemm.** 2005. The TibA adhesin/invasin from enterotoxigenic *Escherichia coli* is self recognizing and induces bacterial aggregation and biofilm formation. Infect. Immun. **73:**1954–1963.

36. **Stalker, D. M., and D. R. Helinski.** 1985. DNA segments of the IncX plasmid R485 determining replication and incompatibility with plasmid R6K. Plasmid **14:**245–254.

37. **Stothard, P., and D. S. Wishart.** 2005. Circular genome visualization and exploration using CGView. Bioinformatics **21:**537–539.

38. **Tenke, P., B. Kovacs, M. Jackel, and E. Nagy.** 2006. The role of biofilm infection in urology. World J. Urol. **24:**13–20.

39. **Ulett, G. C., A. N. Mabbett, K. C. Fung, R. I. Webb, and M. A. Schembri.** 2007. The role of F9 fimbriae of uropathogenic Escherichia coli in biofilm formation. Microbiology **153:**2321–2331.

40. **Valle, J., A. N. Mabbett, G. C. Ulett, A. Toledo-Arana, K. Wecker, M. Totsika, M. A. Schembri, J. M. Ghigo, and C. Beloin.** 2008. UpaG, a new member of the trimeric autotransporter family of adhesins in uropathogenic *Escherichia coli*. J. Bacteriol. **190:**4147–4161.

41. **Valone, S. E., G. K. Chikami, and V. L. Miller.** 1993. Stress induction of the virulence proteins (SpvA, -B, and -C) from native plasmid pSDL2 of *Salmonella dublin*. Infect. Immun. **61:**705–713.

42. **Ward, J. E., D. E. Akiyoshi, D. Regier, A. Datta, M. P. Gordon, and E. W. Nester.** 1988. Characterization of the Virb operon from an Agrobacterium tumefaciens Ti plasmid. J. Biol. Chem. **263:**5804–5814.

43. **Wells, T. J., O. Sherlock, L. Rivas, A. Mahajan, S. A. Beatson, M. Torpdahl, R. I. Webb, L. P. Allsopp, K. S. Gobius, D. L. Gally, and M. A. Schembri.** 2008. EhaA is a novel autotransporter protein of enterohemorrhagic Escherichia coli O157:H7 that contributes to adhesion and biofilm formation. Environ. Microbiol. **10:**589–604.

44. **Williams, S. L., and J. F. Schildbach.** 2006. Examination of an inverted repeat within the F factor origin of transfer: context dependence of F TraI relaxase DNA specificity. Nucleic Acids Res. **34:**426–435.

45. **Wright, K. J., P. C. Seed, and S. J. Hultgren.** 2005. Uropathogenic *Escherichia coli* flagella aid in efficient urinary tract colonization. Infect. Immun. **73:**7657–7668.

46. **Zogaj, X., W. Bokranz, M. Nimtz, and U. Romling.** 2003. Production of cellulose and curli fimbriae by members of the family *Enterobacteriaceae* isolated from the human gastrointestinal tract. Infect. Immun. **71:**4151–4158.